

# Improved Strategy for Direct Instantaneous Torque Control of Switched Reluctance Motors

Chen Zhao<sup>a</sup>, Fujun Deng<sup>b</sup>

School of Automation and Electrical Engineering, Dalian Jiaotong University, Liaoning 116021, China

<sup>a</sup>2103864315@qq.com, <sup>b</sup>1692391556@qq.com

---

## Abstract

In view of the large torque ripple problem of switched reluctance motor (SRM) due to the motor hysteresis control, the BP neural network control strategy is introduced on the basis of the traditional direct instantaneous torque control (DITC) strategy, and the BP neural network adaptive PID is adopted, and the DITC is optimized and adjusted with the square of the torque error as the performance index function. On the basis of the overall double closed-loop control, fuzzy control technology is introduced to improve the speed. Finally, MATLAB/Simulink is used to simulate the traditional DITC and the improved DITC, and the test results show that the improved control strategy can effectively suppress the torque ripple of the switched reluctance motor during operation and control the stable operation of the motor.

## Keywords

Switched Reluctance Motor (SRM); Direct Instantaneous Torque Control (DITC); BP Neural Networks; Fuzzy PID.

---

## 1. Introduction

Switched reluctance motor (SRM) is widely used in the field of electric vehicles because of its solid and simple structure, large starting torque and small starting current. However, the double salient pole structure of SRM and the switching excitation mode cause large instantaneous torque ripple when starting electric vehicles, and even violent jitter and noise, which will affect the stability and comfort of electric vehicles. Therefore, the application of switched reluctance motors in the field of electric vehicles has been limited to a certain extent [1,2].

In order to reduce its torque ripple, scholars at home and abroad propose many improved intelligent algorithms, such as direct instantaneous torque control, neural network control, fuzzy control, torque distribution function control, etc. Literature [3, 4] combines PWM technology with traditional DITC's voltage vector pulse width modulation, and uses torque error to calculate the voltage control vector, which reduces the torque ripple under DITC control, but fails to consider the influence of load and speed on the control effect. Considering the shortcomings of hysteresis controllers, the HYPWM-DITC strategy is proposed, which takes into account the advantages of hysteresis control strategy and PWM, and puts 2 algorithms complement each other. By comparing different position angles for corresponding control, the torque control performance is improved. Literature [6] proposes to introduce fractional order integral and differentiation on the basis of DITC, and the simulation shows that the proposed control strategy improves the response of the system under different working conditions, but will reduce the stability of SMR operation. Literature [7] combines the advantages of RBF neural network and traditional PI control, and introduces PI variable parameters to improve the stability, reliability and speed of control, but compared with other low-phase SRM, its structure

control is too difficult. Literature [8] uses BP neural networks to predict the torque and current characteristics of switched reluctance motors very accurately, but cannot effectively suppress torque ripple. Literature [9] proposes a method for determining torque distribution online, although the influence of load and speed on torque ripple is controlled, but the sampling frequency of the torque loop is too high and the calculation is complicated, and the response speed of the system is also reduced. Literature [10] proposes a control strategy combining dynamic commutation method and wavelet neural network, which can better reduce the torque ripple of SRM\_DITC, adjust the controller parameters under different working conditions, and improve the robustness of the system, but does not consider the complexity of the actual operation of the motor.

Based on the SRM\_DITC strategy, this paper combines fuzzy control and BP neural network PID. The outer ring is a speed ring, which adopts fuzzy control to achieve speed tracking; The inner loop is a torque loop, and the BP neural network PID and DITC direct instantaneous torque control strategy are used to realize torque tracking. The neural network is used to quickly adjust the torque difference and adaptiveness, and effectively suppress the torque ripple.

## 2. SRM\_DITC Strategies

A block diagram of a traditional SRM\_DITC system is shown in Figure 1

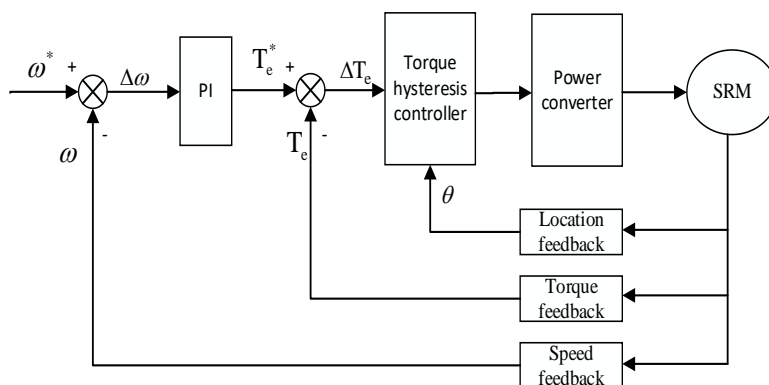


Figure 1. SRM\_DITC system block diagram

The SRM\_DITC system mainly includes PI regulator, torque hysteresis control unit, asymmetric half-bridge power converter, position feedback, torque feedback, speed feedback, motor body and other modules constitute a torque hysteresis control unit. The signal is controlled by the difference between the instantaneous torque and the reference torque and the angle of the current position feedback. The asymmetrical half-bridge power converter applies a different voltage to each phase winding of the motor according to its control instructions to control SRM operation. When the SRM is operating, the legs of each phase winding have three operating states. Taking phase A as an example, the excitation state "1", the freewheeling state "0", and the demagnetization state "-1" are the sequential. The mathematical model of the 6/4 switched reluctance motor used in this paper is analyzed as follows:

- 1)The SRM voltage balance equation is:

$$U = Ri + \frac{d\psi(\theta, i)}{dt} \quad (1)$$

In equation (1),  $U$  is the winding voltage;  $R$  is the winding resistance;  $i$  is the winding current;  $\psi$  is a winding flux linkage;  $\theta$  is the position angle of the stator and rotor.

- 2)The SRM electromagnetic torque equation is:

$$T_e = \frac{1}{2} i^2 \frac{dL}{d\theta} \tag{2}$$

$$T = J \frac{d^2\theta}{dt^2} + B \frac{d\theta}{dt} + T_L \tag{3}$$

In equation (3),  $J$  is the moment of inertia;  $B$  is the coefficient of friction;  $T_L$  is the load torque.

### 3. SRM\_DITC Strategies Fuzzy of BP Neural Network

SRM is a double salient pole structure with severe nonlinear magnetic field distribution, and the commutation power supply in the form of switching makes the traditional PID control strategy unable to effectively control the dynamic and stable performance of the motor. Therefore, this paper introduces fuzzy control and BP neural network intelligent algorithm based on DITC strategy, and the system block diagram is shown in Figure 2.

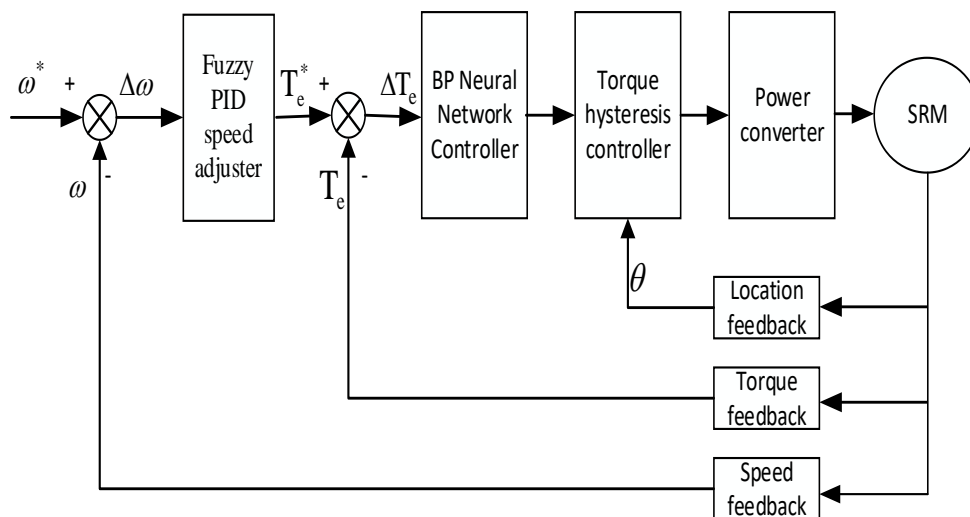


**Figure 2.** Block diagram of SRM\_DITC system based on fuzzy BP neural network

The double closed-loop system mainly includes a velocity outer loop and a torque inner loop. The velocity outer ring consists of a fuzzy PID module, velocity feedback, and position feedback. The deviation between the input speed and the feedback speed of the system is used as the input of the fuzzy control link, and the output is the reference torque; The torque inner loop is composed of BP neural network control module, torque hysteresis loop controller, and torque feedback. The quadratic square of the deviation of reference torque and feedback torque is the performance index function, and the BP neural network PID is used to realize the adjustment of the instantaneous torque, and finally the torque difference controls the working state of the power converter to achieve double closed-loop control.

#### 3.1 Design of Fuzzy Controller

As shown in Figure 3, the fuzzy PID control structure diagram. The fuzzy controller takes the speed error  $e$  and the rate of change of the speed error  $ec$  as the input quantity, and uses fuzzy reasoning to control the parameters and output values to meet  $e$  and  $ec$  to modify the PID parameters of the control system in real time.

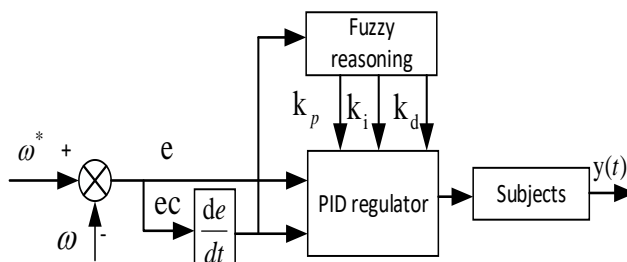


**Figure 3.** Fuzzy PID control structure

3.1.1 Establishment of Membership Functions

Select a triangular function with a relatively uniform distribution according to your specific requirements. Given SRM speed set to 150r/min, Take 150r/min as an example to set the membership function. The basic domain of the input e and ec is [-150,150]. Convert e and ec to fuzzy quantities E and EC, and set the fuzzy domain of input E and EC, output U to [-6,6], and the fuzzy subset of the language values : E , EC = { NB , NM , NS , ZO , PS , PM , PB }, The membership functions of E, EC, and U are shown in Figure 4.

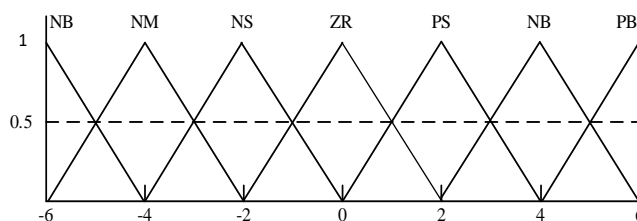


**Figure 4.** Membership functions of E, EC, and U

3.1.2 Fuzzy control rules

Based on the experience of experts, fuzzy rules are obtained. As shown in Table 1, E is the fuzzy set of speed error of the motor, and EC is the fuzzy set of speed error change.

**Table 1.** Two-dimensional fuzzy control rules

U		E						
		NB	NM	NS	ZR	PS	PM	PB
EC	NB	NB	NB	NB	NB	NM	NM	NS
	NM	NB	NB	NB	NM	NS	ZR	ZR
	NS	NB	NB	NM	NS	ZR	ZR	ZR
	ZR	NB	NM	NS	ZR	PS	PM	PB
	PS	ZR	ZR	ZR	ZR	PB	PB	PB
	PM	ZR	ZR	PS	PM	PB	PB	PB
	PB	PS	PM	PB	PB	PB	PB	PB

3.2 Torque Loop Control Strategy

The neural network learning structure adopts three layers 3-4-3, and its structure is shown in Figure 5.

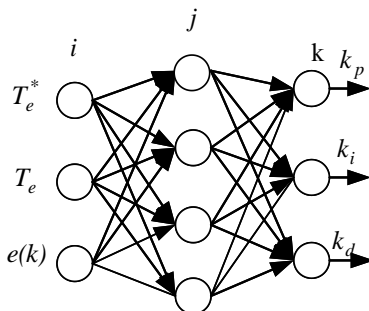


Figure 5. BP network structure

In order to track the reference  $T_e^*$  torque of the switched reluctance motor, the inner loop adopts BP-PID and DITC to control the torque at the same time, and the PID parameters are set by the deviation square of SRM reference torque  $T_e^*$  and feedback torque  $T_e$ . At the same time, the change value of torque deviation is used to adjust the PID parameters, This is shown in Figure 6.

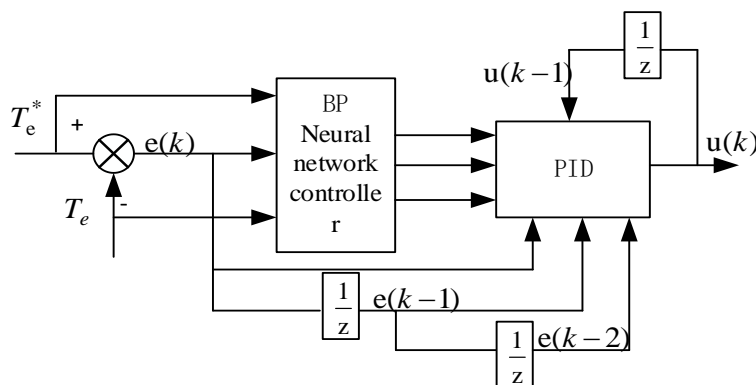


Figure 6. BP neural network control structure

BP neural network is a multilayer feedforward neural network trained according to the error reverse propagation algorithm, and the three parameter values of PID are adjusted online by adjusting the hidden layer threshold.

$$u(k) = u(k-1) + K_p \Delta e(k) + K_i e(k) + K_d e(k) \tag{4}$$

In the formula,  $u(k)$  is the output control quantity of the PID controller,  $K_p$ ,  $K_i$ ,  $K_d$  are proportional, integral, and derivative control parameters, respectively, and  $e(k)$  is the deviation between the system set value and the actual output value.

Deviation of the actual output value.

The network input layer input layer is as follows:

$$O_j^l = X(j) \quad (j=1,2,3) \tag{5}$$

The inputs and outputs of the network hidden layer are:

$$\begin{aligned} net_i^2(k) &= \sum_{j=0}^3 W_{ij}^{(2)} O_j^{(1)}(k) \\ O_i^{(2)}(k) &= f(net_i^2(k)) \end{aligned} \quad (6)$$

where  $W_{ij}^{(2)}$  is the hidden layer weighting coefficient, the upper corner mark corresponds to the three layers of the network, and the corner mark 2 represents the network hidden layer.

Positive and negative symmetric *Sigmoid* hidden layer activation function:

$$f(x) = \frac{1 - e^{-x}}{1 + e^{-x}} \quad (7)$$

The performance indicator function is:

$$\begin{aligned} net_l^3(k) &= \sum_{j=0}^5 W_{lj}^{(3)} O_j^{(2)}(k) \\ O_l^{(3)}(k) &= g(net_l^3(k)) \quad (l = 1, 2, 3) \\ O_1^{(3)} &= K_p, O_2^{(3)} = K_i, O_3^{(3)} = K_d \end{aligned} \quad (8)$$

Output layer activation function:

$$g(x) = \frac{1}{1 + e^{-x}} \quad (9)$$

The performance indicator function is:

$$E(k) = \frac{1}{2} e^2(k) = \frac{1}{2} (r(k) - y(k))^2 \quad (10)$$

where  $r(k)$  is the reference torque signal and  $y(k)$  is the instantaneous torque signal when the motor is running.

Adjust the weight coefficient by the fastest descent method and introduce the inertia term:

$$\Delta W_{ij}^{(3)}(k) = -\eta \frac{\partial E(k)}{\partial W_{ij}^{(3)}} + \alpha \Delta W_{ij}^{(3)}(k-1) \quad (11)$$

where  $\eta$  is the learning rate and  $\alpha$  is the coefficient of inertia.

$$\frac{\partial E(k)}{\partial W_{li}^{(3)}(k)} = \frac{\partial E(k)}{\partial y(k)} \cdot \frac{\partial y(k)}{\Delta u(k)} \cdot \frac{\Delta u(k)}{\partial O_l^{(3)}(k)} \cdot \frac{\partial O_l^{(3)}(k)}{\partial net_l^3(k)} \cdot \frac{\partial net_l^3(k)}{\partial W_{li}^{(3)}(k)} \quad (12)$$

$$\frac{\partial net_l^3(k)}{\partial W_{li}^{(3)}} = O_l^{(2)}(k) \quad (13)$$

Since  $\partial y(k)/\partial \Delta u(k)$  is unknown, the approximation is replaced by the symbolic function  $\text{sgn} [\partial y(k) / \partial \Delta u(k)]$ . Using the incremental PID algorithm, there are:

$$\begin{aligned} \frac{\partial \Delta u(k)}{\partial O_1^{(3)}(k)} &= e(k) - e(k-1) \\ \frac{\partial \Delta u(k)}{\partial O_2^{(3)}(k)} &= e(k) \\ \frac{\partial \Delta u(k)}{\partial O_3^{(3)}(k)} &= e(k) - 2e(k-1) + e(k-2) \end{aligned} \quad (14)$$

Thus, the output layer weight adjustment value is obtained:

$$\begin{aligned} \Delta W_{ii}^{(3)} &= \eta \delta_i^{(3)} \cdot \theta_i^{(2)} + \alpha W_{ii}^{(3)}(k-1) \\ \delta_i^{(3)} &= e(k) \text{sgn}\left(\frac{\partial y(k)}{\partial \Delta u(k)}\right) \frac{\partial \Delta u(k)}{\partial O_1^{(3)}} g'(net_i^{(3)}(k)) \end{aligned} \quad (15)$$

From this, the implied layer weight adjustment can be derived:

$$\begin{aligned} \Delta W_{ij}^{(2)}(k) &= \eta \delta_i^{(2)} O_j^{(1)}(k) + \alpha \Delta W_{ij}^{(2)}(k-1) \\ \delta_i^{(2)} &= f'(net_i^{(2)}(k)) \cdot \sum_{l=1}^3 \delta_l^{(3)} W_{li}^{(3)}(k) \end{aligned} \quad (16)$$

#### 4. Simulation Verification and Analysis

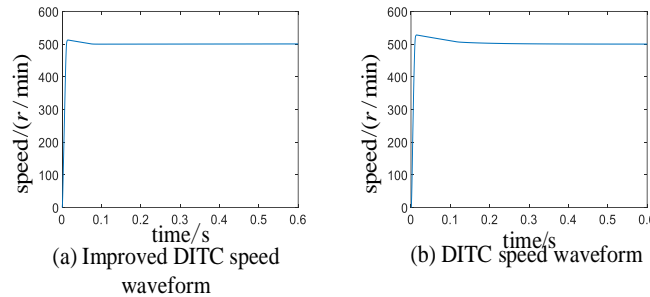
In order to verify the feasibility of the improved SRM\_DITC strategy proposed in this paper. In MATLAB/Simulink, a simulation model is established. In order to reflect the advantages of the improved DITC strategy, the DITC control strategy and the improved DITC strategy are used in the simulation model to compare the variable speed and variable load working conditions of the motor, and the motor simulation parameters are shown in Table 2.

**Table 2.** Motor parameters

Motor parameters	numeric value
type	6/4
Rated power P/(kW)	24
Rated voltage U/(v)	240
Unaligned inductance $L_{\min}$ /(mH)	0.676
Aligned inductance $L_{\max}$ /(mH)	23.6
Stator resistance R/ $\Omega$	0.05
Inertia J/(kg·m <sup>2</sup> )	0.02
Friction B/(N·m·s)	0.02

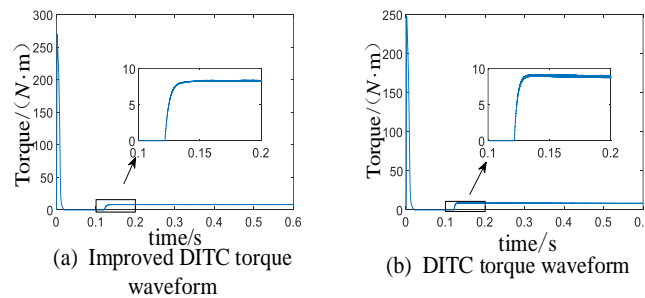
Figure 7 shows the waveform of SRM in no-load state, from startup to stabilization at 500r/min, from the two comparison figures 6(a) and 6(b), it can be seen that the traditional DITC strategy from startup

to stability at 500r/min time is 0.13s, and the improved DITC strategy used in this paper reaches stability at 0.08s. It is shown that the improved DITC control strategy has faster response performance and quickly reaches the rated speed, which verifies the effectiveness of the proposed method.



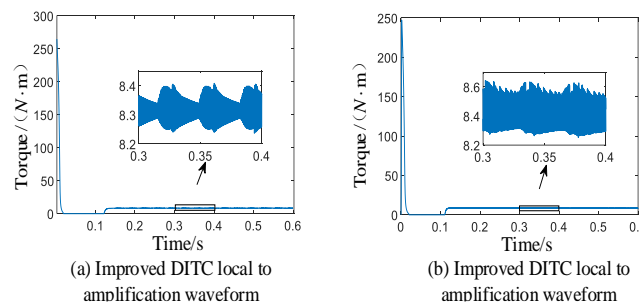
**Figure 7.** RPM waveform of improved DITC and traditional DITC strategies

Figure 8 shows the torque waveform of the improved DITC and traditional DITC strategies. Given a speed of 150r/min, a transition from 0  $N \cdot m$  to 8  $N \cdot m$  occurs at a time of 0.13s, as can be seen from the two comparison figures 7(a) and 7(b), the traditional DITC and improved DITC reach stability at 0.15s, but the torque of the improved strategy is more stable during the transition process, which verifies the anti-interference of the proposed method.



**Figure 8.** Torque waveform of improved DITC and traditional DITC strategies

Figure 9 shows the improved DITC and traditional DITC torque local amplification waveforms. When the motor is between 0.3 and 0.4s in the stable operation stage, the improved torque wave amplitude is between 8.2 and 8.4  $N \cdot m$ , which is better than the traditional DITC's 8.2 and 8.65  $N \cdot m$ . From the simulation waveform results, it can be seen that the improved strategy suppresses torque ripple to a certain extent.



**Figure 9.** improves the torque local amplification waveform for DITC and traditional DITC

Define the torque ripple coefficient  $K_t$  as follows:



$$K_t = (T_{max} - T_{min}) / T_{av} \quad (17)$$

$T_{max}$ ,  $T_{min}$  and  $T_{av}$  are the maximum torque, minimum torque, and average torque when SRM reaches stability.

The parameters after reaching stability are shown in Table 3, the traditional DITC torque ripple coefficient is about 0.04295, and the improved DITC torque ripple coefficient is about 0.0197, which is about 2.2 times lower than the original, and the results show that the improved torque ripple is relatively small.

**Table 3.** Comparison of torque ripple coefficients

	$T_{max}$	$T_{min}$	$T_{av}$	$K_t$
DITC	8.65	8.287	8.45	0.04295
Improve DITC	8.4	8.24	8.32	0.0197

## 5. Conclusion

- (1) The traditional DITC control method, because the internal mathematical model of SRM is difficult to accurately determine, cannot determine the problem of control parameters. In this paper, the composite control method is used to solve this problem, and the response ability of direct instantaneous torque control is improved, and the anti-interference ability of the system is enhanced.
- (2) By comparing the simulation results of the traditional SRM\_ DITC system, it is confirmed that the torque ripple suppression effect is better in the new system, the system dynamic, static and robust performance are better, and the torque ripple is well solved.

## References

- [1] WANG Lei,XIE Yan,LU Qinghui. Design and research of speed control system of switched reluctance motor for electric vehicle[J].South China Agricultural Machinery,2022,53(05):13-15.
- [2] LI Yitao. Review of torque ripple suppression of switched reluctance motor[J]. Electric Machine Technology,2019,(06):53-58.
- [3] Pestana L M, Calado M R A, Mariano S. Direct instantaneous thrust control optimization of a linear switched reluctance actuator by pulse-width modulation duty ratio adjustment[C]/ IEEE 14th International Conference on Environment and Electrical Engineering ( EEEIC) ,Roma,Italy,2014: 464-468.
- [4] Wang H,Lee D H,Ahn J W. Torque ripple reduction of SRM using advanced direct instantaneous torque control scheme[C]/ International Conference on Electrical Machines and Systems( ICEMS) ,Seoul, Korea,2007: 492-496.
- [5] CHENG Yong,CAO Xiaoxiao,ZHANG Yilong. Direct instantaneous torque control of switched reluctance motor hysteresis-pulse width modulation[J].Electric Machines and Control,2020,24(08):74-82.
- [6] Party Election, Peng Huimin, Jiang Hui, et al. Direct instantaneous torque control of switched reluctance motor based on fuzzy fractional order PID[J].Journal of Vibration and Shock,2018,37(23):104-110.
- [7] GAO Yu,DAI Yuehong,SONG Lin. Modeling of switched reluctance motor based on BP neural network[J].Power Electronics,2017,51(02):72-74.
- [8] HU Chunlong. Research on direct torque control system of five-phase switched reluctance motor based on neural network[J].Machinery and Electronics,2021,39(08):36-40.
- [9] Jin Y,Bilgin B,Emadi A. An extended-speed lowripple torque control of switched reluctance motor drives [J].IEEE Transactions on Power Electronics,2015,30(3) : 1457-1470.
- [10] Jin Aijuan, Liu Jianpeng, Li Shaolong. Control method of switched reluctance motor based on dynamic commutation strategy[J].Information and Control,2022,51(06):730-740.